Intereye Comparison of Lamina Cribrosa Curvature in Normal Tension Glaucoma Patients With Unilateral Damage

Jeong-Ah Kim,[1] Tae-Woo Kim,[2] Eun Ji Lee,[2] Joon Mo Kim,[3] Michaël J. A. Girard,[4,5] and Jean Martial Mari[6]

[1]Department of Ophthalmology, Hallym University College of Medicine, Chuncheon Sacred Heart Hospital, Chuncheon, Korea
[2]Department of Ophthalmology, Seoul National University College of Medicine, Seoul National University Bundang Hospital, Seongnam, Korea
[3]Department of Ophthalmology, Kangbuk Samsung Hospital, Sungkyunkwan University School of Medicine, Seoul, Korea
[4]Department of Biomedical Engineering, National University of Singapore, Singapore
[5]Singapore Eye Research Institute, Singapore National Eye Centre, Singapore
[6]Université de la Polynésiefrançaise, Tahiti, French Polynesia

Correspondence: Tae-Woo Kim, Department of Ophthalmology, Seoul National University Bundang Hospital, 82, Gumi-ro, 173 Beon-gil, Bundang-gu, Seongnam, Gyeonggi-do 463-707, Korea; twkim7@snu.ac.kr.
Joon Mo Kim, Department of Ophthalmology, Kangbuk Samsung Hospital, Sungkyunkwan University School of Medicine, 29 Saemunan-ro, Jongno-gu, Seoul 03181, Korea; kjoonmo1@gmail.com.

Submitted: February 7, 2019
Accepted: April 25, 2019

Citation: Kim J-A, Kim T-W, Lee EJ, Kim JM, Girard MJA, Mari JM. Intereye comparison of lamina cribrosa curvature in normal tension glaucoma patients with unilateral damage. *Invest Ophthalmol Vis Sci*. 2019;60:2423–2430. https://doi.org/10.1167/iovs.19-26828

Purpose. To investigate intereye differences in lamina cribrosa (LC) morphology in normal tension glaucoma (NTG) patients with unilateral damage.

Methods. A total of 152 eyes of 76 treatment-naive NTG patients with unilateral damage from the ongoing Investigating Glaucoma Progression Study were included. Optic nerve heads were scanned using enhanced-depth spectral-domain optical coherence tomography. The magnitude of the LC curve and LC position were assessed by measuring the LC curve index (LCCI) and LC depth (LCD), respectively, at seven locations spaced equidistantly across the vertical optic disc diameter. LCCI and LCD were compared between glaucomatous and fellow healthy eyes.

Results. Eyes with NTG had larger average LCCI and LCD than contralateral healthy eyes (for both $P < 0.002$). The LCCI was greater in the glaucomatous eyes at all seven locations ($P < 0.001$). Univariate conditional logistic regression analysis showed that higher baseline intraocular pressure ($P = 0.010$), deeper LCD ($P = 0.007$), and larger LCCI ($P < 0.001$) were significantly associated with the presence of glaucoma. In multivariate analysis, only larger LCCI was significantly associated with the presence of glaucoma ($P < 0.001$).

Conclusions. Glaucomatous eyes have more steeply curved LC than fellow healthy eyes. This finding suggests that LC undergoes significant remodeling in NTG eyes.

Keywords: normal tension glaucoma, lamina cribrosa, lamina cribrosa curve index

Glaucoma is an optic neuropathy characterized by progressive loss of retinal ganglion cells (RGCs) and their axons. Although elevated intraocular pressure (IOP) is a strong risk factor for glaucoma,[1] IOP is not elevated in over half of untreated glaucoma patients in many regions.[2–6] Moreover, a large proportion of patients with ocular hypertension do not develop glaucoma over several years of follow-up.[7] Therefore, the pathogenesis of glaucoma and the role of IOP in its pathogenesis remain to be elucidated.

According to mechanical theory, changes in lamina cribrosa (LC) morphology are important in the development of glaucoma associated with elevated IOP. Postmortem examination of glaucoma patients with high IOP showed that the LC was posteriorly bowed and compressed.[8] In addition, an experimental study in an early glaucoma model showed that changes in LC preceded loss of the retinal nerve fiber layer (RNFL) after IOP elevation.[9] The deformed LC are thought to promote damage of axons and its cell body (RGC) through diverse mechanisms, including a blockade of axonal transport and connective tissue remodeling by reactive astrocytes.[10–12] Furthermore, compression of the LC may affect the diffusion of nutrients from the capillaries inside the laminar beams to the adjacent axons, thereby further compromising the axons.[13]

Efficacy of IOP-lowering treatment to retard glaucoma progression has been proven in normal tension glaucoma (NTG) patients,[14] indicating that IOP also plays an important role in NTG. However, the precise mechanism of how the IOP-related stress is involved in NTG remains largely unknown. In this regard, it would be of interest to examine the LC morphology, which is known to be a key factor in glaucoma pathogenesis, in NTG. If LC strain is involved in the pathogenesis of NTG, NTG eyes would have a LC feature implying a more severely deformed configuration (e.g., more steeply curved LC) than healthy eyes.

Glaucoma is considered to be a multifactorial disease in which both localized ocular (e.g., IOP[1]) and systemic factors (e.g., blood pressure,[15] cold extremities,[16] sleep apnea,[17] etc.) are involved. This makes it complicated to identify a pathogenic factor/mechanism of glaucomatous optic nerve damage through a comparison among individuals. In this regard,

intereye comparison within an individual has an advantage in determining the role of ocular factors such as LC morphology because influences from systemic factors would be applied equally to both eyes. Furthermore, IOP-lowering treatment may induce change in the LC morphology in glaucomatous eyes.[18–22] Therefore, we compared LC morphology between eyes in treatment-naive NTG patients with unilateral damage in an attempt to elucidate whether LC strain is related to the pathogenesis of NTG.

Methods

This cross-sectional analysis involved patients enrolled between January 2012 and March 2017 in the ongoing Investigating Glaucoma Progression Study (IGPS),[23,24] a prospective clinical trial approved by the Seoul National University Bundang Hospital Institutional Review Board. The protocol of the present study was in accordance with the Declaration of Helsinki for biomedical research involving human subjects.

Study Subjects

Patients enrolled in the IGPS underwent a complete ophthalmic examination, including measurements of best corrected visual acuity (BCVA); refraction tests; slit-lamp biomicroscopy; Goldmann applanation tonometry; gonioscopy; dilated stereoscopic examination of the optic disc; measurements of corneal curvature (KR-1800; Topcon, Tokyo, Japan), central corneal thickness (Orbscan II; Bausch & Lomb Surgical, Rochester, NY, USA), and axial length (IOL Master version 5; Carl Zeiss Meditec, Dublin, CA, USA); stereo disc photography (EOS D60 digital camera; Canon, Utsunomiya-shi, Tochigi-ken, Japan); spectral-domain optical coherence tomography (SD-OCT) (Spectralis; Heidelberg Engineering, Heidelberg, Germany); and standard automated perimetry (Humphrey Field Analyzer II 750 and 24-2 Swedish interactive threshold algorithm; Carl Zeiss Meditec).

The IGPS excluded subjects with a history of intraocular surgery other than cataract extraction and glaucoma surgery, any intraocular disease (e.g., diabetic retinopathy or retinal vein occlusion), or any neurologic disease (e.g., stroke or brain tumor) that could cause visual field (VF) loss; and subjects with BCVA worse than 20/40.

All patients included in the IGPS had regular follow-up every 3 to 6 months with slit-lamp examinations using a 78-diopter (D) lens or stereo disc photography. SD-OCT RNFL thickness was measured at intervals ranging from 6 to 24 months. Patients included in the present study were required to be treatment naive at the time of optic nerve head (ONH) scan and to have unilateral manifest NTG (i.e., NTG with VF defect in one eye and healthy fellow eye).

NTG was diagnosed according to the following criteria: IOP $\leq$ 21 mm Hg on multiple measurement on the same day or over a few days before starting IOP-lowering medication, an open angle on gonioscopy, glaucomatous optic nerve damage (e.g., the presence of diffuse or localized rim thinning, notching, or a disc hemorrhage), and associated VF defects without ocular disease or conditions that may cause VF abnormalities. A glaucomatous VF change was defined as the fulfillment of two or more of the following criteria: (1) outside normal limits on the glaucoma Hemifield test; (2) three abnormal points with <5% probability of being normal, including one with a probability <1%, by pattern deviation; or (3) a pattern standard deviation (PSD) of probability <5%. These VF defects were confirmed on two consecutive reliable tests (fixation loss rate $\leq$20%, false-positive and false-negative error rates $\leq$25%). The contralateral eye had to have an open angle on gonioscopy, IOPs of $\leq$21 mm Hg during the follow-up period, a normal-appearing optic disc, and a normal VF. A healthy eye was defined when the optic disc was healthy looking without glaucomatous change and the VF result was normal.

Eyes were excluded if they had a BCVA worse than 20/40, a spherical equivalent less than –6.0 or greater than +3.0 D, a cylinder correction of less than –3.0 or greater than +3.0 D, a tilted disc (i.e., a tilt ratio between the longest and shortest diameters of the optic disc of >1.3),[25,26] or a torted disc (i.e., a torsion angle deviation of the long axis of the optic disc from the vertical meridian of >15°).[26,27] Eyes were also excluded if a good-quality image (i.e., quality score >15) could not be obtained in more than five sections. If the quality score did not reach 15, the image-acquisition process automatically stopped or images of the respective sections were not obtained. Only acceptable scans with good-quality images that allowed clear delineation of the anterior border of the LC within the Bruch's membrane opening (BMO) were included to measure the LC depth (LCD) and the LCCI.

IOP was measured diurnally every 2 hours from 9:00 AM to 5:00 PM (five measurements) on the same day or on different days, prior to administration of IOP-lowering medication, and the average of the five measurements was defined as the baseline IOP. The ONH was imaged by SD-OCT using enhanced-depth imaging (EDI) technique on the same day that baseline IOP was measured.

EDI-OCT of the ONH and Adaptive Compensation

The LCD and degree of LC curve were measured using optic disc B-scan images, which were obtained using the EDI technique of the SD-OCT system with a high speed setting.[28] Prior to disc scanning, the corneal curvature of each eye was entered into the Spectralis OCT system to avoid potential magnification errors. The optic disc was imaged through undilated pupils using a rectangle subtending 10° × 15° of the optic disc. This rectangle was scanned with approximately 75 B-scan section images that were separated by 30 to 34 μm (the distance between the scan lines was determined automatically). An average of approximately 42 SD-OCT frames were obtained for each section. This protocol provided the best trade-off between image quality and patient cooperation.[29]

To enhance the visibility of the anterior LC surface, all disc scan images were post processed using adaptive compensation,[30–32] and the measurements were performed using a manual caliper tool in the software (Amira, version 5.2.2; Visage Imaging, Berlin, Germany) by two experienced observers (J.A.K. and E.J.L.) who were masked to the clinical information. If the anterior LC surface was not visualized clearly, an adjacent horizontal EDI-OCT scan, approximately 30 to 35 μm apart from the original scan, was used for measurement. When the anterior LC surface was not visualized even in the adjacent scans, we excluded that eye. The average LCD and LCCI were the means of the measurements taken at seven points of the LC. The mean of the measurements made by the two observers was used for analysis.

Measurement of LCD

The LCD was measured at seven locations equidistant across the vertical optic disc diameter using horizontal SD-OCT B-scan images. These seven B-scan lines were defined as planes 1 to 7 (superior to inferior regions, Fig. 1A). In this model, plane 4 corresponds to the midhorizontal plane, and planes 2 and 6 correspond to the superior and inferior midperiphery planes, respectively. To determine the LCD, a line connecting the

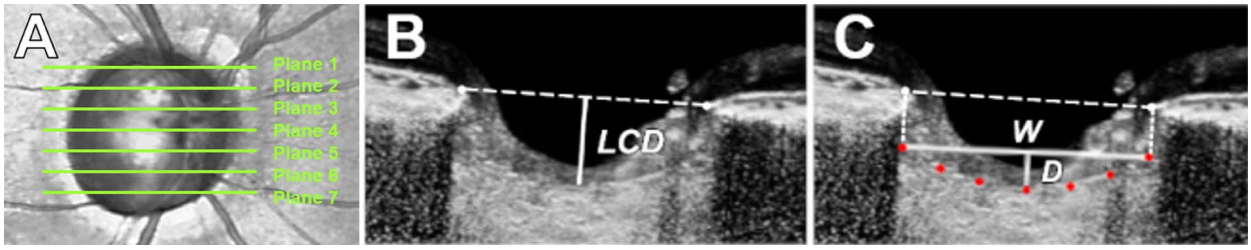

Figure 1. Measurements of the LCD and LCCI. (**A**) Infrared fundus image of an eye with lines indicating the levels of the seven B-scan images spaced equidistantly across the vertical optic disc diameter. (**B**) Measurement of the LCD from the reference line connecting the two BMO points to the anterior surface of the LC. The LCD was measured as the distance from this reference line at the maximally depressed point. (**C**) The LCCI was measured by dividing the LC curve depth (D) within the BMO by the width of the anterior LC surface reference line (W), and then multiplying by 100.

edges of the BMO was set as the reference plane (BMO reference line), and the LCD was measured in the direction perpendicular to the reference plane at the maximally depressed point (Fig. 1B).

Measurement of LC Curve

The LC curve was assessed with the LCCI using EDI SD-OCT images. The method used to calculate LCCI has been described previously.[20,33–37] In brief, LCCI was determined by measuring the width of the LC curve reference line (LCCW) and then measuring the LC curve depth (LCCD). The LCCW was defined as the width of the line connecting the two points on the anterior LC surface that met with lines drawn from each BMO termination point perpendicular to the BMO reference line. The maximum depth from the reference line to the anterior LC surface was defined as the LCCD (Fig. 1C). The LCCI was calculated as (LCCD/LCCW) × 100. Because the curvature is normalized relative to LC width, it describes the shape of the LC independent of the actual size of the ONH. Only the LC within the BMO was considered because the LC was often not clearly visible outside the BMO. In eyes with LC defects, the LCCI and LCD were measured using a presumed anterior LC surface that best fit the curvature of the remaining part of the LC or excluded the area of the LC defect.

Table 1. Demographic Characteristics of the Study Subjects ($n = 76$)

Variables	Unilateral Manifest NTG		
	Glaucomatous Eye	Healthy Eye	*P* Value
Age, y	57.8 ± 11.7		
Female gender (%)	36 (47.4)		
Diabetes mellitus (%)	9 (11.8)		
Hypertension (%)	27 (35.5)		
Family history of glaucoma (%)	8 (10.5)		
Cold extremities (%)	9 (11.8)		
Migraine (%)	6 (7.9)		
Baseline IOP, mm Hg	13.9 ± 2.6	13.3 ± 2.5	**0.003**
Spherical error, D	−0.81 ± 2.03	−0.62 ± 1.97	**0.013**
Central corneal thickness, µm	551.3 ± 37.2	541.8 ± 70.6	0.208
Axial length, mm	24.05 ±1.07	24.00 ± 1.03	0.052
Vertical cup-to-disc ratio	0.65 ± 0.14	0.50 ± 0.09	**<0.001**
RNFL thickness, µm			
Global	78.8 ± 13.9	94.1 ± 9.3	**<0.001**
Superior sector	96.1± 24.8	113.8 ± 14.3	**<0.001**
Nasal sector	61.4 ± 12.7	66.0 ± 11.2	**<0.001**
Inferior sector	92.4 ± 26.5	122.6 ± 16.4	**<0.001**
Temporal sector	65.1 ± 11.6	74.0 ± 10.1	**<0.001**
Automated perimetry, dB			
MD	−5.38 ± 4.25	−0.58 ± 1.30	**<0.001**
PSD	6.13 ± 3.86	1.86 ± 0.66	**<0.001**
Average BMO width, µm	1456.4 ± 124.3	1445.6 ± 136.8	0.213

Data are mean ± standard deviation or *n* (%) values. Factors with statistical significance are shown in bold. MD, mean deviation.

Statistical Analysis

Data were expressed as mean ± SD except where otherwise indicated. The interobserver agreement for measuring LCCI and LCD was evaluated by calculating the 95% Bland-Altman limits of agreement. Categorical variables were compared between groups using χ^2 tests, and continuous variables were compared using paired *t*-tests. Univariate and multivariate conditional logistic regression analyses were performed to identify factors associated with the presence of glaucoma. Variables with *P* values <0.1 on univariate analysis were included in the multivariate analysis, and backward variable selection was utilized to obtain the final multivariable model. Probability values of $P < 0.05$ were considered statistically significant. All statistical analyses were performed using software (Statistical Package for the Social Sciences version 22.0; SPSS, Chicago, IL, USA).

Results

Baseline Characteristics

This study initially involved 91 patients diagnosed with NTG with unilateral damage. Of these, 15 patients were excluded because the image quality of their SD-OCT disc scans was too poor to allow clear visualization of their anterior LC surfaces. Of the remaining 76 patients, 40 (52.6%) were men. Mean patient age was 57.8 ± 11.7 years. Table 1 shows the clinical characteristics of these patients. Glaucomatous eyes had a higher baseline IOP (13.9 ± 2.6 vs. 13.3 ± 2.5 mm Hg, $P = 0.003$), thinner global RNFL thickness (78.8 ± 13.9 vs. 94.1 ± 9.3 µm, $P < 0.001$), and worse VF mean deviation (MD) (–5.38 ± 4.25 vs. –0.58 ± 1.30 dB, $P < 0.001$) and PSD (6.13 ± 3.86 vs. 1.86 ± 0.66 dB, $P < 0.001$) than contralateral healthy eyes of these patients. In contrast, there were no significant intereye differences in central corneal thickness (551.3 ± 37.2 vs. 541.8 ± 70.6 µm, $P = 0.208$), axial length (24.05 ± 1.07 vs. 24.00 ± 1.03 mm, $P = 0.052$), and average BMO width (1456.4 ± 124.3 vs. 1445.6 ± 136.8, $P = 0.213$).

Table 2. Comparison of the LCD and LCCI Between Glaucomatous Eyes and Fellow Healthy Eye in Unilateral Naive NTG Patients ($n = 76$)

	LCD, μm			LCCI		
Plane Number	**Glaucomatous Eye**	**Healthy Eye**	***P* Value**	**Glaucomatous Eye**	**Healthy Eye**	***P* Value**
1	531.9 ± 107.4	514.9 ± 109.1	**0.015**	9.17 ± 1.67	7.97 ± 1.41	**<0.001**
2	556.1 ± 122.1	523.2 ± 113.9	**<0.001**	9.69 ± 2.12	7.82 ± 2.02	**<0.001**
3	541.7 ± 122.0	513.2 ± 114.4	**<0.001**	9.01 ± 2.32	7.37 ± 1.79	**<0.001**
4	505.8 ± 120.8	487.2 ± 116.4	**0.013**	8.35 ± 2.05	7.04 ± 1.77	**<0.001**
5	482.3 ± 125.5	470.7 ± 108.5	0.260	8.12 ± 2.16	7.22 ± 1.66	**<0.001**
6	483.0 ± 108.7	464.0 ± 101.1	**0.022**	10.16 ± 2.29	8.26 ± 1.65	**<0.001**
7	464.3 ± 105.5	455.5 ± 102.5	0.223	9.87 ± 2.36	8.01 ± 1.67	**<0.001**
Average	509.3 ± 109.5	489.8 ± 102.8	**0.002**	9.28 ± 1.62	7.67 ± 1.31	**<0.001**

Data are mean ± standard deviation values, with statistically significant *P* values in boldface.

Comparison of LCD and LCCI

The 95% Bland-Altman limits of agreement for the measurements of LCD and LCCI between the measurements from the two glaucoma specialists were –31.16 to 31.47 μm and –1.16 to 1.17, respectively. The mean differences were 0.15 μm for the LCD and 0.01 for the LCCI.

Table 2 and Figure 2 show comparisons of LCD and LCCI in NTG and healthy eyes. Compared with their contralateral healthy eyes, glaucomatous eyes had a significantly higher mean LCD (509.3 ± 109.5 vs. 489.8 ± 102.8 μm, $P = 0.002$) and LCCI (9.28 ± 1.62 vs. 7.67 ± 1.31, $P < 0.001$). The LCCIs in all seven planes were significantly higher in glaucomatous than in healthy eyes (all *P* values < 0.001; Fig. 3 and Table 2).

Factors Associated With the Presence of Glaucoma

Table 3 shows the results of conditional logistic regression analysis assessing factors associated with the presence of glaucoma. Univariate analysis showed that higher baseline IOP (odds ratio [OR], 1.750; 95% confidence interval [CI] = 1.144, 2.67; $P = 0.010$), higher LCD (OR, 1.017; 95% CI = 1.005, 1.030, $P = 0.007$), and higher LCCI (OR, 11.622; 95% CI =3.552, 38.032; $P < 0.001$) were significantly associated with the presence of glaucoma. On multivariate analysis, however, only LCCI was significantly associated with the presence of glaucoma (OR, 11.62; 95% CI = 3.552, 38.032, $P < 0.001$).

Representative Case

Figure 4 shows a NTG patient with unilateral damage who had a larger LCCI in the glaucomatous eye than in the contralateral healthy eye.

Discussion

The present study demonstrated that NTG eyes had more steeply curved LCs and larger LCDs than did fellow healthy eyes. In addition, the LCCI was a significant lateralizing factor for unilateral glaucomatous damage. To our knowledge, there has been no study in the literature comparing LC morphology between eyes of treatment-naive NTG patients with unilateral damage.

According to the mechanical theory of glaucoma, IOP-related stress induces morphologic changes or remodeling of the load-bearing ONH connective tissues,[13,38] resulting in posterior bowing[9,39] and/or displacement of LC insertion.[40,41] Eyes that undergo these changes would have larger LCCI and LCD. Based on this assumption, the results of the current study suggest that the LC strain is involved in NTG patients despite their IOP being within the normal range.

Our finding that the LC is more steeply curved in glaucomatous eyes than in contralateral normal eyes is of particular interest because, in the present study, the mean IOP was only 0.6 mm Hg greater in glaucomatous eyes than in healthy eyes. The mechanisms underlying the intereye

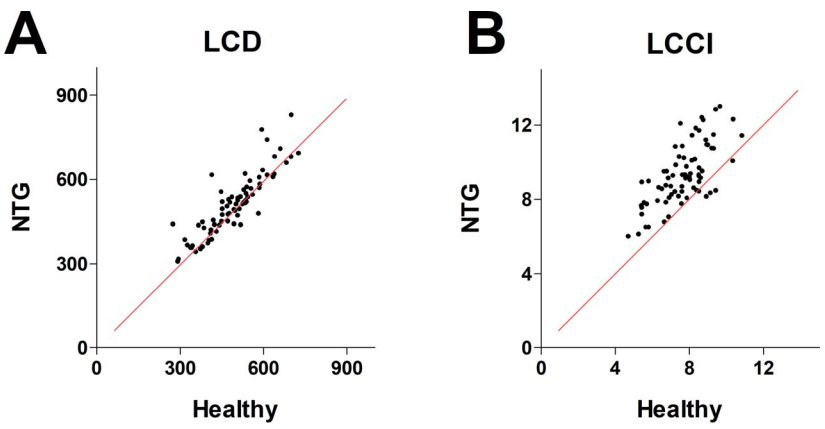

Figure 2. Scatter plots showing comparisons of the LCD (**A**) and LCCI (**B**) in NTG and contralateral healthy eyes in patients with NTG with unilateral damage. Most NTG eyes had a deeper LCD and a larger LCCI than did fellow healthy eyes. The *red lines* indicate equivalence between NTG and healthy eyes.

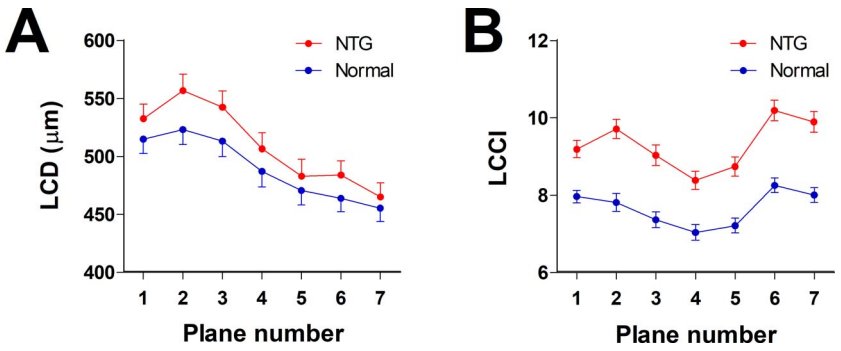

FIGURE 3. Comparison of the LCD (**A**) and LCCI (**B**) in seven horizontal EDI SD-OCT scans of glaucomatous and contralateral healthy eyes. Planes 1 and 7 correspond to the superior- and inferior-most planes, respectively. The LCCIs were larger at all seven planes in glaucomatous than in healthy eyes ($P < 0.001$ each), whereas the LCDs were deeper at planes 1, 2, 3, 4, and 6 in glaucomatous than in healthy eyes ($P < 0.05$ each).

difference in LCCI remain unclear. A possible hypothesis is that the intereye difference in LC morphology is innate. If this is the case, our data suggest that eyes with larger LCCI may be more susceptible to glaucomatous damage. Further study is warranted to investigate whether posteriorly bowed LC increases the susceptibility of axons to IOP-induced stress. Second possible hypothesis is that the retrolaminar tissue pressure may be different between eyes. Unilateral or highly asymmetric papilledema, which is not rare in patients with increased intracranial pressure,[42,43] is considered to be due to a difference in cerebrospinal fluid pressure between right and left optic nerve sheaths.[43] Thus, retrolaminar tissue pressure may not be equal between the eyes of any individual. This may be accompanied by a translaminar pressure difference (TLPD) between eyes, despite comparable IOP, leading to greater LCCI in one side. Alternatively, the tissue properties of the LC may differ between eyes, resulting in differences in resistance to IOP or TLPD.[13] Related to this, it is noteworthy that the LCCI has a regional variability within an individual eye, and the area of larger LCCI corresponds to the location of axonal loss in eyes with hemifield VF defect.[34] Since the IOP is the same, the regional variability within an individual eye is probably affected by the material property of the LC at that region.[44] The finding suggests that posterior LC deformation first occurs at the location with material property of highest susceptibility to LC deformation, leading to subsequent development of axonal damage at the corresponding location.[33,34] If a method to measure the material property of LC becomes available, this hypothesis can be tested.

It may be argued that the LC deformation may be a secondary change to axonal loss. However, we regard this possibility as unlikely for the following reasons. Studies employing experimental glaucoma models generated by an IOP elevation have demonstrated that LC deformation occurs prior to a detectable loss of the RNFL loss.[9] In contrast, posterior LC deformation was not observed in an optic nerve crush model[45] or nonglaucomatous optic neuropathy,[46,47] both of which suffered substantial loss of RNFL. Moreover, we recently demonstrated that larger LCCI had a predictability for a faster rate of RNFL loss in glaucoma-suspect patients.[33] Furthermore, the LCCI is not correlated with glaucoma severity in the primary open-angle glaucoma patient,[37] supporting that LCCI is not a secondary change to axonal loss. If LC bowing occurs secondarily, larger degree of LCCI would be observed in eyes with more advanced-stage disease.

Univariate analysis showed that both the LCD and LCCI were lateralizing factors for the presence of NTG. However, only LCCI remained significant in the multivariate analysis. This may be due to the collinearity between LCD and LCCI, with the LCCI having a greater effect. This is in line with previous studies, which demonstrated that the LCCI could better distinguish between glaucomatous and healthy eyes.[37] The LCD, which is measured from the BMO reference plane, is affected by choroidal thickness, a parameter that varies among individuals.[48,49] In contrast, the LCCI is independent of choroidal thickness. We recently demonstrated that the LCCI better predicts the future rate of RNFL thinning than LCD in eyes with suspected glaucoma[33] and open-angle glaucoma,[36] further suggesting that LCCI is a better marker of glaucomatous LC strain.

Consistent with previous studies,[15,28,34] the LCD was largest in the superior planes (Fig. 3; Table 2). This was likely due to the choroidal thickness being thicker superiorly than inferiorly.[50] In contrast, the LCCI was largest in the two most inferior planes, in agreement with results showing that the inferotemporal sector was the most frequent location of RNFL damage in glaucoma patients.[37,51]

Studies have demonstrated that IOP lowering can effectively prevent or retard glaucoma progression.[14,52] Our finding that the LC is more steeply curved in NTG than in normal eyes,

TABLE 3. Factors Associated With the Presence of Glaucoma in Unilateral NTG Patients (n=76)

	Univariate Analysis			Multivariate Analysis*		
Variables	**OR**	**95% CI**	***P* Value**	**OR**	**95% CI**	***P* Value**
Baseline IOP, per 1 mm Hg higher	1.750	1.144–2.676	**0.010**	1.109	0.498–2.471	0.800
Spherical error, per 1 D larger	0.386	0.172–0.868	**0.021**	1.082	0.117–10.022	0.945
CCT, per 1 μm thicker	1.008	0.992–1.024	0.316			
Axial length, per 1 mm longer	10.828	0.847–138.338	0.067	10.140	0.002–53709.319	0.596
Average LCD, per 1 μm deeper	1.017	1.005–1.030	**0.007**	1.011	0.978–1.044	0.528
Average LCCI, per 1 larger	11.622	3.552–38.032	**<0.001**	11.62	3.552–38.032	**<0.001**

Factors with statistical significance are shown in bold. OR, odds ratio; CI, confidence interval; CCT, central corneal thickness.
* Variables with $P < 0.1$ in the univariate analysis were included in the multivariate model.

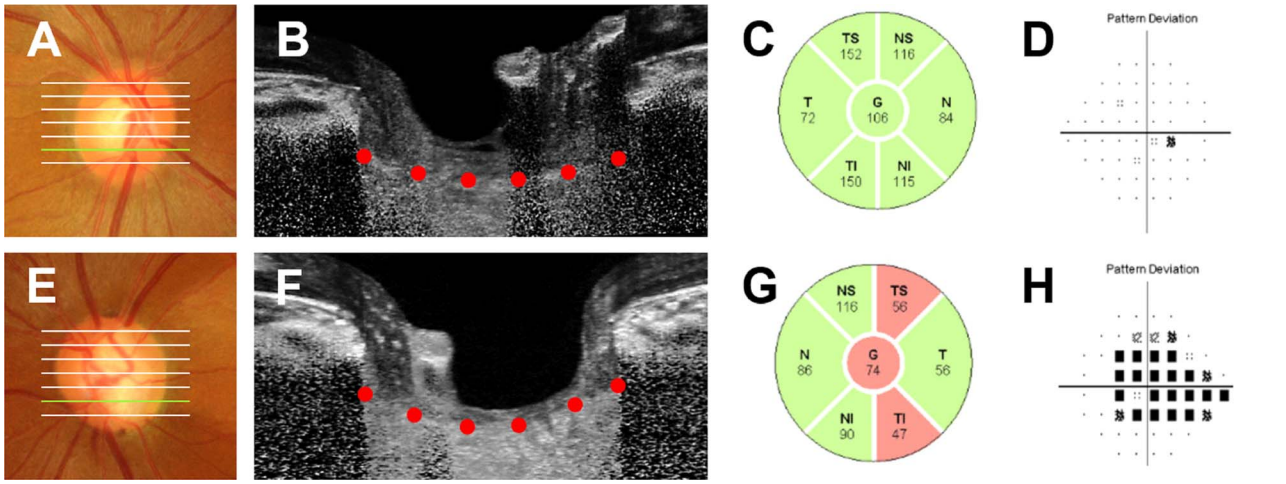

Figure 4. A 52-year-old woman with unilateral treatment-naive NTG in her left eye. Her untreated intraocular pressure was 13 mm Hg OD and 15 mm Hg OS, and her central corneal thickness was 527 µm OD and 533 µm OS. Disc photos, circumpapillary RNFL thickness profiles, and VF pattern deviation plots confirm the presence of glaucomatous damage in the left (**E**–**H**), but not in the right eye (**A**–**D**). The glaucomatous eye had more steeply curved LC (**F**) than did the contralateral healthy eye (**B**) at the inferior midperipheral plane, which corresponds to the site of disc rim loss area in the left eye (**E**).

hence likely being associated with IOP-induced strain, is in line with results showing that IOP lowering can slow glaucoma progression in NTG eyes.[14] However, it is unclear whether stresses and strains induced by IOP are the most important pathogenic factors in all eyes with NTG, as LC curves in some NTG eyes have been reported to have comparable LC curves to those in healthy eyes.[35] IOP in these NTG eyes was lower, with these eyes having greater parapapillary structural alterations and systemic risk factors.[35] Recently, Park et al.[53] reported a positive correlation between prelamina tissue thickness and parapapillary choroidal thicknesses in treatment-naive NTG patients. Moreover, the prelamina tissue thickness was related to the severity of glaucomatous damage. These findings indicate that choroidal blood flow may be related to the pathogenesis of NTG independent of the pathogenic process related to mechanical stress. In the current study, some patients had a comparable to or even smaller LCCI in NTG than in contralateral healthy eyes, suggesting that non-IOP–related factors such as ONH blood supply may play a more significant role in glaucoma development in these eyes.

Akkaya et al.[54] have reported that diabetic patients had thicker and more anteriorly positioned LC compared to healthy controls. Of the 76 patients included in the present study, nine (11.8%) had diabetes mellitus (DM). However, we did not address the effect of DM on LC position in this analysis. This was because the effect of DM would have been intrinsically controlled by the study design, which was an intereye comparison within an individual. Therefore, the effect of DM would be applied in both groups simultaneously.

This study had several limitations. First, an LC surface reference line relative to the LC insertion points would allow more precise quantification of the LC curve. In the present study, however, only the LC within the BMO width was included in the measurement of LC curves, as the LC was often not visible outside this region. We previously demonstrated that the LCCI measured from the entire LC (i.e., between the LC insertions) was comparable to that measured on the LC within BMO in eyes with an LC visible up to the LC insertion.[20] Thus, assessment of the LC curve within BMO was considered comparable to the assessment of the actual LC curve. Second, the LCCI does not correspond to the actual LC curvature but is only an approximation. Further studies are needed to investigate the optimal method of calculating the real LC curvature. Third, eyes with a tilted or torted optic disc were excluded, precluding application of the reported findings to eyes with these conditions. Lastly, all patients in this study were Korean. Therefore, these results may not be directly applicable to patients of other ethnicities.

In conclusion, the present study found that the LC was more steeply curved in glaucomatous than in contralateral healthy eyes of patients with treatment-naive NTG with unilateral damage. In addition, the degree of LC curvature was significantly associated with the presence of glaucoma. This finding suggests that LC undergoes significant remodeling in NTG eyes.

Acknowledgments

Disclosure: **J.-A. Kim**, None; **T.-W. Kim**, None; **E.J. Lee**, None; **J.M. Kim**, None; **M.J.A. Girard**, None; **J.M. Mari**, None

References

1. Weinreb RN, Aung T, Medeiros FA. The pathophysiology and treatment of glaucoma: a review. *JAMA*. 2014;311:1901–1911.
2. Rotchford AP, Johnson GJ. Glaucoma in Zulus: a population-based cross-sectional survey in a rural district in South Africa. *Arch Ophthalmol*. 2002;120:471–478.
3. Shen SY, Wong TY, Foster PJ, et al. The prevalence and types of glaucoma in Malay people: the Singapore Malay eye study. *Invest Ophthalmol Vis Sci*. 2008;49:3846–3851.
4. Suzuki Y, Iwase A, Araie M, et al. Risk factors for open-angle glaucoma in a Japanese population: the Tajimi Study. *Ophthalmology*. 2006;113:1613–1617.
5. Liang YB, Friedman DS, Zhou Q, et al. Prevalence of primary open angle glaucoma in a rural adult Chinese population: the Handan eye study. *Invest Ophthalmol Vis Sci*. 2011;52:8250–8257.
6. Kim M, Kim TW, Park KH, Kim JM. Risk factors for primary open-angle glaucoma in South Korea: the Namil study. *Jpn J Ophthalmol*. 2012;56:324–329.
7. Kass MA, Heuer DK, Higginbotham EJ, et al. The Ocular Hypertension Treatment Study: a randomized trial determines that topical ocular hypotensive medication delays or prevents the onset of primary open-angle glaucoma. *Arch Ophthalmol*. 2002;120:701–713; discussion 829–730.

8. Quigley HA, Addicks EM, Green WR, Maumenee AE. Optic nerve damage in human glaucoma. II. The site of injury and susceptibility to damage. *Arch Ophthalmol*. 1981;99:635–649.
9. Bellezza AJ, Rintalan CJ, Thompson HW, Downs JC, Hart RT, Burgoyne CF. Deformation of the lamina cribrosa and anterior scleral canal wall in early experimental glaucoma. *Invest Ophthalmol Vis Sci*. 2003;44:623–637.
10. Anderson DR, Hendrickson A. Effect of intraocular pressure on rapid axoplasmic transport in monkey optic nerve. *Invest Ophthalmol Vis Sci*. 1974;13:771–783.
11. Minckler DS, Bunt AH, Johanson GW. Orthograde and retrograde axoplasmic transport during acute ocular hypertension in the monkey. *Invest Ophthalmol Vis Sci*. 1977;16:426–441.
12. Hernandez MR. The optic nerve head in glaucoma: role of astrocytes in tissue remodeling. *Prog Retin Eye Res*. 2000;19:297–321.
13. Burgoyne CF, Downs JC, Bellezza AJ, Suh JK, Hart RT. The optic nerve head as a biomechanical structure: a new paradigm for understanding the role of IOP-related stress and strain in the pathophysiology of glaucomatous optic nerve head damage. *Prog Retin Eye Res*. 2005;24:39–73.
14. Collaborative Normal-Tension Glaucoma Study Group. Comparison of glaucomatous progression between untreated patients with normal-tension glaucoma and patients with therapeutically reduced intraocular pressures. *Am J Ophthalmol*. 1998;126:487–497.
15. Leske MC, Heijl A, Hyman L, et al. Predictors of long-term progression in the early manifest glaucoma trial. *Ophthalmology*. 2007;114:1965–1972.
16. Nicolela MT, Ferrier SN, Morrison CA, et al. Effects of cold-induced vasospasm in glaucoma: the role of endothelin-1. *Invest Ophthalmol Vis Sci*. 2003;44:2565–2572.
17. Mojon DS, Hess CW, Goldblum D, et al. High prevalence of glaucoma in patients with sleep apnea syndrome. *Ophthalmology*. 1999;106:1009–1012.
18. Lee EJ, Kim TW, Weinreb RN, Kim H. Reversal of lamina cribrosa displacement after intraocular pressure reduction in open-angle glaucoma. *Ophthalmology*. 2013;120:553–559.
19. Rebolleda G, de Juan V, Munoz-Negrete FJ, Diez-Alvarez L. Simultaneous evaluation of the lamina cribosa position and choroidal thickness changes following deep sclerectomy. *Eur J Ophthalmol*. 2018;28:662–669.
20. Lee SH, Yu D-A, Kim T-W, Lee EJ, Girard MJ, Mari JM. Reduction of the lamina cribrosa curvature after trabeculectomy in glaucoma. *Invest Ophthalmol Vis Sci*. 2016;57:5006–5014.
21. Lee EJ, Kim TW, Weinreb RN. Reversal of lamina cribrosa displacement and thickness after trabeculectomy in glaucoma. *Ophthalmology*. 2012;119:1359–1366.
22. Lee EJ, Kim TW, Weinreb RN. Variation of lamina cribrosa depth following trabeculectomy. *Invest Ophthalmol Vis Sci*. 2013;54:5392–5399.
23. Kim YW, Lee EJ, Kim TW, Kim M, Kim H. Microstructure of beta-zone parapapillary atrophy and rate of retinal nerve fiber layer thinning in primary open-angle glaucoma. *Ophthalmology*. 2014;121:1341–1349.
24. Choi YJ, Lee EJ, Kim BH, Kim TW. Microstructure of the optic disc pit in open-angle glaucoma. *Ophthalmology*. 2014;121:2098–2106.
25. Jonas JB, Papastathopoulos KI. Optic disc shape in *glaucoma*. *Graefes Arch Clin Exp Ophthalmol*. 1996;234(suppl 1):S167–173.
26. Vongphanit J, Mitchell P, Wang JJ. Population prevalence of tilted optic disks and the relationship of this sign to refractive error. *Am J Ophthalmol*. 2002;133:679–685.
27. Samarawickrama C, Mitchell P, Tong L, et al. Myopia-related optic disc and retinal changes in adolescent children from Singapore. *Ophthalmology*. 2011;118:2050–2057.
28. Spaide RF, Koizumi H, Pozonni MC. Enhanced depth imaging spectral-domain optical coherence tomography. *Am J Ophthalmol*. 2008;146:496–500.
29. Lee EJ, Kim TW, Weinreb RN, Park KH, Kim SH, Kim DM. Visualization of the lamina cribrosa using enhanced depth imaging spectral-domain optical coherence tomography. *Am J Ophthalmol*. 2011;152:87–95.
30. Girard MJ, Tun TA, Husain R, et al. Lamina cribrosa visibility using optical coherence tomography: comparison of devices and effects of image enhancement techniques. *Invest Ophthalmol Vis Sci*. 2015;56:865–874.
31. Girard MJ, Strouthidis NG, Ethier CR, Mari JM. Shadow removal and contrast enhancement in optical coherence tomography images of the human optic nerve head. *Invest Ophthalmol Vis Sci*. 2011;52:7738–7748.
32. Strouthidis N, Mari JM, Park SC, Girard M. Enhancement of lamina cribrosa visibility in optical coherence tomography images using adaptive compensation. *Invest Ophthalmol Vis Sci*. 2013;54:2149–2149.
33. Kim JA, Kim TW, Weinreb RN, Lee EJ, Girard MJA, Mari JM. Lamina cribrosa morphology predicts progressive retinal nerve fiber layer loss in eyes with suspected glaucoma. *Sci Rep*. 2018;8:738.
34. Kim JA, Kim TW, Lee EJ, Girard MJA, Mari JM. Lamina cribrosa morphology in glaucomatous eyes with hemifield defect in a Korean population [published ahead of print December 24, 2018]. *Ophthalmology*. https://doi.org/10.1016/j.ophtha.2018.12.042.
35. Lee SH, Kim TW, Lee EJ, Girard MJA, Mari JM, Ritch R. Ocular and clinical characteristics associated with the extent of posterior lamina cribrosa curve in normal tension glaucoma. *Sci Rep*. 2018;8:961.
36. Lee EJ, Kim T-W, Kim H, Lee SH, Girard MJ, Mari JM. Comparison between lamina cribrosa depth and curvature as a predictor of progressive retinal nerve fiber layer thinning in primary open-angle glaucoma. *Ophthalmol Glaucoma*. 2018;1:44–51.
37. Lee SH, Kim T-W, Lee EJ, Girard MJ, Mari JM. Diagnostic power of lamina cribrosa depth and curvature in glaucoma. *Invest Ophthalmol Vis Sci*. 2017;58:755–762.
38. Yan DB, Coloma FM, Metheetrairut A, Trope GE, Heathcote JG, Ethier CR. Deformation of the lamina cribrosa by elevated intraocular pressure. *Br J Ophthalmol*. 1994;78:643–648.
39. Yang H, Ren R, Lockwood H, et al. The connective tissue components of optic nerve head cupping in monkey experimental glaucoma part 1: global change. *Invest Ophthalmol Vis Sci*. 2015;56:7661–7678.
40. Yang H, Williams G, Downs JC, et al. Posterior (outward) migration of the lamina cribrosa and early cupping in monkey experimental glaucoma. *Invest Ophthalmol Vis Sci*. 2011;52:7109–7121.
41. Lee KM, Kim TW, Weinreb RN, Lee EJ, Girard MJ, Mari JM. Anterior lamina cribrosa insertion in primary open-angle glaucoma patients and healthy subjects. *PLoS One*. 2014;9:e114935.
42. Lepore FE. Unilateral and highly asymmetric papilledema in pseudotumor cerebri. *Neurology*. 1992;42:676–678.
43. Wall M, White WN II. Asymmetric papilledema in idiopathic intracranial hypertension: prospective interocular comparison of sensory visual function. *Invest Ophthalmol Vis Sci*. 1998;39:134–142.
44. Quigley HA, Dorman-Pease ME, Brown AE. Quantitative study of collagen and elastin of the optic nerve head and sclera in human and experimental monkey glaucoma. *Curr Eye Res*. 1991;10:877–888.

Investigative Ophthalmology & Visual Science

45. Ing E, Ivers KM, Yang H, et al. Cupping in the monkey optic nerve transection model consists of prelaminar tissue thinning in the absence of posterior laminar deformation. *Invest Ophthalmol Vis Sci*. 2016;57:2914–2927.
46. Fard MA, Afzali M, Abdi P, et al. Optic nerve head morphology in nonarteritic anterior ischemic optic neuropathy compared to open-angle glaucoma. *Invest Ophthalmol Vis Sci*. 2016;57:4632–4640.
47. Lee EJ, Choi YJ, Kim TW, Hwang JM. Comparison of the deep optic nerve head structure between normal-tension glaucoma and nonarteritic anterior ischemic optic neuropathy. *PLoS One*. 2016;11:e0150242.
48. Johnstone J, Fazio M, Rojananuangnit K, et al. Variation of the axial location of Bruch's membrane opening with age, choroidal thickness, and race. *Invest Ophthalmol Vis Sci*. 2014;55:2004–2009.
49. Rhodes LA, Huisingh C, Johnstone J, et al. Variation of laminar depth in normal eyes with age and race. *Invest Ophthalmol Vis Sci*. 2014;55:8123–8133.
50. Jiang R, Wang YX, Wei WB, Xu L, Jonas JB. Peripapillary choroidal thickness in adult Chinese: The Beijing Eye Study. *Invest Ophthalmol Vis Sci*. 2015;56:4045–4052.
51. Leung CK, Choi N, Weinreb RN, et al. Retinal nerve fiber layer imaging with spectral-domain optical coherence tomography: pattern of RNFL defects in glaucoma. *Ophthalmology*. 2010;117:2337–2344.
52. Heijl A, Leske MC, Bengtsson B, et al. Reduction of intraocular pressure and glaucoma progression: results from the Early Manifest Glaucoma Trial. *Arch Ophthalmol*. 2002;120:1268–1279.
53. Park JH, Yoo C, Jung JH, Girard MJA, Mari JM, Kim YY. The association between prelaminar tissue thickness and peripapillary choroidal thickness in untreated normal-tension glaucoma patients. *Medicine (Baltimore)*. 2019;98:e14044.
54. Akkaya S, Kucuk B, Dogan HK, Can E. Evaluation of the lamina cribrosa in patients with diabetes mellitus using enhanced depth imaging spectral-domain optical coherence tomography. *Diab Vasc Dis Res*. 2018;15:442–448.

Investigative Ophthalmology & Visual Science